MEASUREMENT OF PLASMA PARAMETERS FOR COPPER USING LASER INDUCED BREAKDOWN SPECTROSCOPY

A. SAFEEN[a,*], W. H. SHAH[a], R. KHAN[a], A. SHAKEEL[a], Y. IQBAL[a], G. ASGHAR[a], R. KHAN[b], G. KHAN[b], K. SAFEEN[b], W. H. SHAH[c]
[a]*Department of Physics, University of Poonch, Rawalakot, 12350, Pakistan*
[b]*Department of Physics, Abdul Wali Khan University, 23200, Mardan, Pakistan*
[c]*Department of Physics , International Islamic University, Islamabad, Pakistan*

In this study, we present Laser Induced-Breakdown Spectroscopy (LIBS) of Copper with a Neodymium-doped yttrium aluminum garnet (Nd: YAG) laser having wavelength 532 nm and laser energy 400 mJ. We calculated the plasma temperature by Boltzmann plot method for various copper transition ($3d^94s^2 \rightarrow 3d^{10}5p$) at 261.89 nm ($3d^94s^2 \rightarrow 3d^94s4p$) at 282.44 nm ($3d^94s^2 \rightarrow 3d^94s4p$) at 296.14 nm ($3d^{10}4s \rightarrow 3d^{10}4p$) at 324.79 nm ($3d^{10}4s \rightarrow 3d^{10}4p$) 327.38 nm ($3d^94s4p \rightarrow 3d^94s4d$) 330.79 nm ($3d^94p \rightarrow 3d^95s$) at 268.96 nm ($3d^94d \rightarrow 3d^95f$) at 329.02 nm and ($3d^84s4p \rightarrow 3d^95d$) at 528.98 nm. The plasma density is determined by stark broadening profile of the peak corresponding to wavelength 528.98 nm and to transition ($3d^84s4p \rightarrow 3d^95d$). Identification of transition lines from spectrum was carried out by comparing spectral lines with NIST atomic data base. We further studied the variation of the plasma temperature and plasma density by changing the distance between sample under consideration and laser source. We also investigated the plasma temperature and plasma density variation with different laser irradiance flux.

(Received October 17, 2018; Accepted January 10, 2019)

Keywords: Laser induced breakdown spectroscopy, Copper plasma, Stark broadening

1. Introduction

In laser induced spectroscopy (LIBS), a plasma is generated on the surface of a target by focusing a laser beam. Laser beam excites and ionizes the target material. The emission of plasma begins on the surface of target soon after the laser photon reaches on the target surface [1]. Optical detection of certain atomic and molecular species is obtained by analyzing their emission spectra from laser-induced plasma. LIBS is a type of analytical technique of atomic emission spectroscopy with which any type of matter whether in liquid, solid or gaseous state can be analyzed [2-9]. The choice of experimental conditions strongly affects the analytical performance of LIBS. Parameters like wavelength of laser light used, laser pulse energy, pulse duration, observation time duration, ambient gas pressure, type and properties of target, and the geometric setup of the optical instruments used strongly influence the performance of LIBS [10]. Runge and Minck [11], and Rusak *et al*. [12] made the first direct spectral analysis by using LIBS. This technique gained increasing importance as an analytical technique in research in the 1980’s [13]. It becomes important to study laser-induced plasmas of metal alloys as they have many interesting and important applications, *e,g.*, materials processing, device fabrication, thin film deposition, *etc.* Copper in its elemental form, being a good metal conductor, finds its many applications in different areas like electronic and electrical engineering. After the development of LIBS technique, copper plasma has been studied by many researchers in different aspects over the years [14-25]. Kumar and Thareja [26] investigated the spatial and temporal behavior of the copper plasma produced by laser in vacuum and in the presence of neon and argon gases as well.

In this work, we have studied spatial evaluation of copper plasma produced by LIBS Nd: YAG laser having wavelength and laser pulse energy 532 nm and 400 mJ respectively. The experimentally observed copper transition lines are used for determination of plasma temperature

[*] Corresponding author: akifsafeen@upr.edu.pk

(T_e) by Boltzmann plot method whereas, electron number density (N_e) was determined using Cu-I at 528.98 nm from Stark broadening parameter. Then we studied the plasma temperature and electron number density variation with distance from target to laser pulses source. We also investigated the variation in plasma temperature and electron number density with laser flux energy in air at atmospheric pressure.

2. Experimental setup

The LIBS experimental setup is shown in Fig. 1. We have used a Q-switched Nd:YAG (Quantel Brilliant) single pulsed laser of energy 400 mJ at 532 nm to generate plasma of target sample to avoid delay mechanism and for storing the spectrum of first laser generated plasma. A Joule meter (Nova-Quante 101507) was used to measure the pulse energy. A convex lens of focal length 20 cm was used to focus the laser beam on the target which was mounted on three-dimensional stage capable of rotation to avoid the non-uniform pitting of the sample. To avoid any breakdown of air in front of the sample, focusing lens and the sample were separated by a distance less than the focal length of the lens. A high-OH fiber optics (core diameter of 600 mm) with a collimating lens was placed at right angle to the laser beam direction to collect the radiation emitted by the plasma. Plasma emission was measured by connecting the optical fiber to the LIBS 2000 detection system (Ocean Optics Inc.). The detection system consists of five spectrometers covering a range of wavelength between 220 nm and 720 nm. Each spectrometer has a 5 mm wide slit. There is a time delay of about 3 ms between the laser pulse and the start of data recording. The emission spectrum data is recorded through a synchronization between Q-switched Nd:YAG laser and LIBS-2000 detection system. Detection system was triggered by flash lamp of Nd:YAG laser through four-chanel pulse generator (SRSDG535) and the Q-switch of the Nd:YAG laser was triggered by the LIBS-2000 detection system.

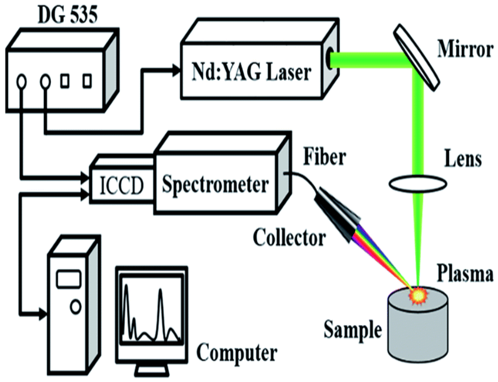

Fig. 1. Experimental setup of LIBS system.

3. Results and discussions

3.1. Emission studies

In the current work, we have studied the copper plasma produced using a Q-switched Nd:YAG laser at 532 nm wavelength with a pulse energy of 400 mJ. Shock waves are produced causing the plasma produced by high intensity laser pulse to expand normal to the target surface [27]. The emission spectra of copper plasma produced at the surface of target were recorded at different distances along the expansion of plasma plume.

Table 1. Spectroscopic parameters for spectral lines identification of copper.

Ions	Wavelength λ (nm)	Transition probability A_k s^{-1} (10^7)	Statistical weight		Transition levels	Upper level energy $E_k(cm^{-1})$
			g_i	g_k		
Copper I (Cu I)						
Cu-I	261.89	3.07	4	6	$3d^94s^2\ ^2D_{5/2}\rightarrow 3d^{10}5p\ ^2P^o_{3/2}$	49382.94
Cu-I	282.44	0.7	6	6	$3d^94s^2\ ^2D_{5/2}\rightarrow 3d^94s4p\ ^2D^o_{5/2}$	46598.35
Cu-I	296.14	0.36	8	6	$3d^94s^2\ ^2D5/2\rightarrow 3d^94s4p\ ^2F^o_{7/2}$	44963.26
Cu-I	324.79	13.95	4	2	$3d^{10}4s\ ^2S_{1/2}\rightarrow 3d^{10}4p\ ^2P^o_{3/2}$	30783.69
Cu-I	327.38	13.8	2	2	$3d^{10}4s\ ^2S_{1/2}\rightarrow 3d^{10}4p\ ^2P^o_{1/2}$	30535.32
Cu-I	330.79	22.2	12	10	$3d^94s4p\ ^4F^o_{9/2}\rightarrow 3d^94s4d\ ^4G_{11/2}$	71130.68
Copper II (Cu II)						
Cu-II	268.96	5.9	7	7	$3d^94p\ ^1F^o_3\rightarrow 3d^9(^2D_{5/2})5s\ ^2[5/2]_3$	108014.83
Cu-II	329.02	5.9	13	11	$3d^9(^2D_{5/2})4d\ ^2[9/2]_5\rightarrow 3d^9(^2D_{5/2})5f\ ^2[11/2]^o_6$	145951.53
Cu-II	528.98		9	7	$3d^8(^3F)4s4p(^3P^o)\ ^3F^o_3\rightarrow 3d^9(^2D_{5/2})5d\ ^2[7/2]_4$	137044.46

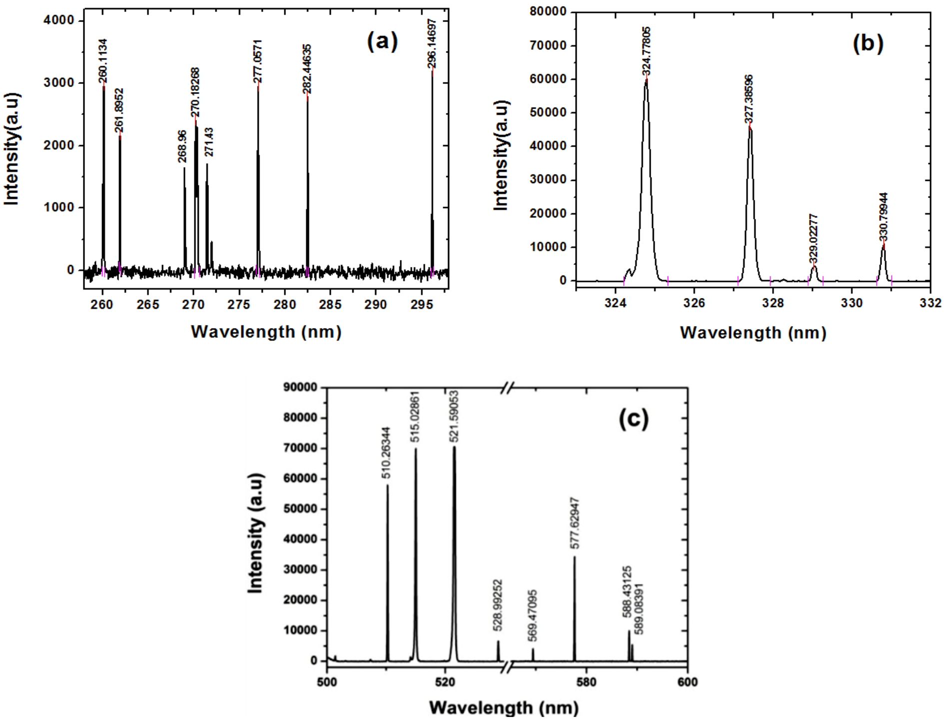

Fig. 2. Copper spectrum generated by the Nd:YAG laser 532 nm having energy 400 mJ in the region (a) 250-300 nm, (b) 322-332 nm (c) 500-600 nm.

Fig. 2 (a), (b) and (c) show the emission spectra of copper over the spectral range between 200–600 nm. Most of the dominating lines belong to emission corresponding to neutral copper while some emissions are due to singly ionized copper plasma. The observed spectral lines of copper Cu-I are identified as 261.89 ($3d^94s^2\ ^2D_{5/2}\rightarrow 3d^{10}5p\ ^2P^o_{3/2}$), 282.44 ($3d^94s^2\ ^2D_{5/2}\rightarrow 3d^94s4p\ ^2D^o_{5/2}$), 296.14 ($3d^94s^2\ ^2D5/2\rightarrow 3d^94s4p\ ^2F^o_{7/2}$), 324.79 ($3d^{10}4s\rightarrow 3d^{10}4p$), 324.79 ($3d^{10}4s\ ^2S_{1/2}\rightarrow$

$3d^{10}4p\ ^2P^o_{3/2}$), 327.38 ($3d^{10}4s\ ^2S_{1/2} \rightarrow 3d^{10}4p\ ^2P^o_{1/2}$) and 330.79 nm ($3d^94s\ 4p\ ^4F^o_{9/2} \rightarrow 3d^94s4d\ ^4G_{11/2}$). Similarly the observed spectral lines of Cu-II are identified as 268.96 ($3d^94p\ ^1F^o_3 \rightarrow 3d^9(^2D_{5/2})5s\ ^2[5/2]_3$), 329.02 ($3d^9(^2D_{5/2})4d\ ^2[9/2]_5 \rightarrow 3d^9(^2D_{5/2})5f\ ^2[11/2]^o_6$) and 528.99 nm ($3d^8(^3F)4s4p(^3P^o)\ ^3F^o_3 \rightarrow 3d^9(^2D_{5/2})5d\ ^2[7/2]_4$). Spectral lines are identified by using NIST database system [28]. The identified lines of copper along with other spectroscopic parameters are presented in Table 1. All these identified copper spectral lines and its plasma parameters are used to find plasma temperature and electron number density.

3.2. Measurement of plasma temperature and electron number density

The well resolved spectral lines of copper were used to extract the plasma parameters, particularly plasma temperature (T_e) and electron number density (N_e). Electron temperature and electron number density are known to be independent of each other and the condition of local thermodynamic equilibrium must be satisfied for the validity of Boltzmann relationship. This condition allows to find the temperature varying from place to place. Generally, the plasma temperature can be found out by three methods namely (i) Two lines method (ii) Saha-Boltzmann and (iii) Boltzmann plot method. We used Boltzmann plot methods to calculate the plasma temperature as given by following equation [29].

$$\ln\left(\frac{\lambda I}{hcAg}\right) = -\frac{\Delta E}{kT_e}, \qquad \text{Slope} = -\frac{1}{kT_e}. \tag{1}$$

where 'I' is the spectral line intensity of the emission line,'ΔE' is the difference between two energy level, 'T_e' is the plasma electron temperature, 'k' is the Boltzmann constant,'h' is plank's constant,'c' is the speed of light, 'A' is the transition probability, 'g' is the statistical weight of the level and 'λ' is the wavelength of spectral lines. A plot of $\ln(\lambda I / Ag)$ versus energy ΔE gives straight line with slope equal to $-1/kT_e$. The plasma temperature is determined by graph slope which is in the range 12000–13000 K. The different spectroscopic parameters for identified lines of copper, taken from NIST database, are listed in Table 1. Variation of electron temperature as a function of distance from the target surface has also been studied for Nd:YAG laser at 532 nm. It has been observed that electron temperature varies from 13520 K to 12250 K as the distance is changed from 0.5 mm to 8 mm from target surface along the direction of plasma plume as shown in Fig. 3(a). It has been observed that electron temperature near target surface is higher than the for end of the system. This is due to constantly absorption of radiation during the interaction of laser pulse by means of electron via the inverse bremsstrahlung's absorption process [30]. The electron temperature decreases with increasing distance due to rapidly conversion of thermal energy into kinetic energy. When plasma gains maximum expansion velocities, drop in electron temperature occurs for plasma expansion. Decreasing electron temperature with distance from the target has been reported by Ying *et al.* [31] for ArF excimer laser irradiance and by Lindner *et al.* [32] in case of laser-particle interaction in LIBS and laser ablation inductively coupled plasma spectrometry.

Local thermodynamic condition (LTE) requires the minimum electron number density which can be determined by the equation [33-35].

$$N_e \geq 1.6\times10^{12} T_e^{1/2} (\Delta E)^3 . \tag{2}$$

$T(K)$ represents the electron temperature and ΔE (eV) is the difference in energy between the two states. The width of a spectral line can also be used to determine the electron number density. Broadening in the spectral lines of plasma is mainly due to doppler broadening and stark broadening [36]. The Doppler width can be calculated by using the following relation [31].

$$\Delta\lambda = \lambda\sqrt{\frac{8kT\ln 2}{Mc^2}} . \tag{3}$$

where M is the molecular weight. Considering only the electron contribution to the line broadening and neglecting the contribution of ion broadening, the stark broadening line width $\Delta\lambda_{1/2}$ (FWHM) can be estimated by the relation:

$$\Delta\lambda_{1/2} = 2\omega \left(\frac{N_e}{10^{16}}\right) . \tag{4}$$

where ω is the electron impact width parameter. Equation (4) is used to calculate the electron number density of the spectral line.

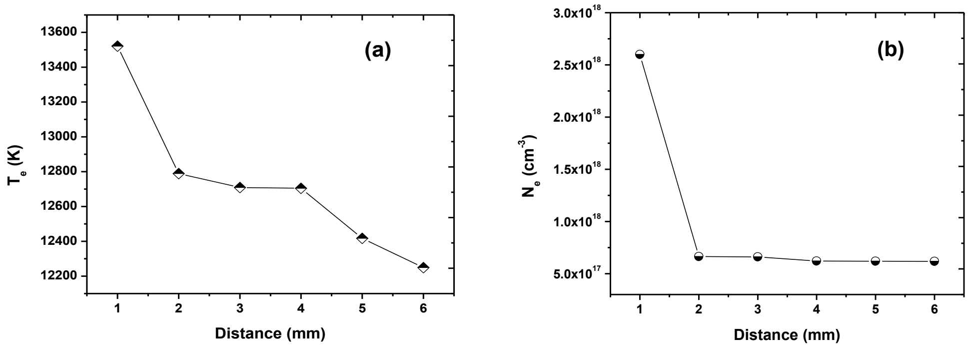

Fig. 3. Variation of (a) electron temperature (b) electron number density with distance.

The electron number density near the surface of the target is found to be $2.5938 \times 10^{18} cm^{-3}$. The variation of electron density as a function of distance from target along the direction of plasma expansion is shown in Fig. 3(b). We observed that the electron number density varies with distance in the direction of plasma evolution. Electron number density has a maximum value near target surface and it decreases as laser source is moved away from target. The decrease in electron number density with distance is two fold; first it decreases sharply $2.5938 \times 10^{18} cm^{-3}$ to $6.6281 \times 10^{17} cm^{-3}$ and then decreases steadily from $6.6281 \times 10^{17} cm^{-3}$ to $6.1832 \times 10^{17} cm^{-3}$. The decrease in electron number density can be attributed to recombination process in the region where plasma is expanded [30].

3.3. Variation of plasma temperature and electron number density with laser energy

We also calculated the plasma temperature and electron number density for various energy flux of Nd:YAG laser (532 nm). We observed that widths and intensities of identified spectral lines are directly related to laser energy and both quantities are directly proportional to each other. The plasma temperature is calculated by changing the laser pulse energy from 50–400 mJ in Nd:YAG (532 nm). The observed plasma temperature varies from about 11400–12800K as shown in Fig. 4(a). We also calculated electron number density for various laser energy values, which is directly proportional to the laser energy. The electron number density increases from $3.4801\times10^{15} cm^{-3}$ to $6.1179\times10^{17} cm^{-3}$ as laser energy is increased from 50–400 mJ as shown in Fig. 4(b). Higher value of electron number density at lower wavelength (higher energy) of laser irradiance indicates higher mass ablation rate. Similar trend of electron number density with laser irradiance wavelength is reported by H. Lindner *et al.* [32] and D. Gunther *et al.* [37]. When laser energy is increased, more ions and free electrons are produced. Due to interaction of ions and free electrons with incoming laser beam, more ionization and heating is produced which causes more consumption of incident laser energy. The variation in plasma electron temperature and electron number density with change in laser energy may be due to reflection or absorption of laser photons by the plasma depending on the frequency [30, 36].

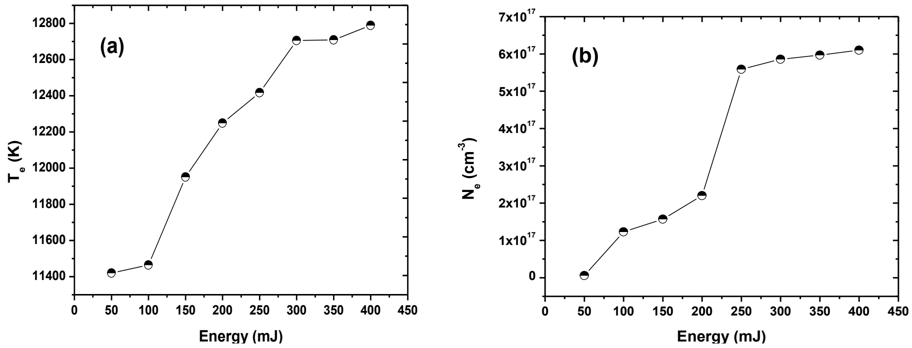

Fig. 4. Variation of (a) Electron temperature and (b) Electron number density with energy.

4. Conclusions

In this study the copper plasma is produced by using LIBS through Q-switched Nd:YAG laser at 532 nm wavelength with an energy of 400 mJ. Transitions of singly ionized and neutral copper have been observed in the plasma emission spectrum. Plasma temperature is calculated by Boltzmann plot which is in the range 12000–13000 K. The electron number density near copper surface is calculated by Stark broadening parameter which comes out to be in the range between 2.5938 $\times 10^{18} cm^{-3}$ and $6.1832 \times 10^{17} cm^{-3}$. We found that spatial behavior of plasma temperature and electron number density close to the target is larger and both of these quantities decrease with distance from the sample along the axial direction of plasma plume. From the study of the variation of the plasma temperature and electron number density with the laser energy we conclude that both these quantities increase with the increase of the laser energy.

References

[1] S. S. Harilal, C. V. Bindhu, M. S. Tillack, F. Najmabadi, A. C. Gaeris, J. Appl. Phys. **93**, 2380 (2003).
[2] N. M. Shaikh, S. Hafeez, B. Rashid, M. A. Baig, Eur. Phys. J. D **44**, 371 (2007).
[3] J. A. Aguilera, C. Aragon, F. Penalba, Appl. Surf. Sci. **309**, 127 (1998).
[4] D. A. Cremers, L. J. Radziemski, T. R. Loree, Appl. Spectrosc. **38**, 72 (1984).
[5] V. N. Rai, F. Y. Yueh, J. P. Singh, Appl. Opt. **42**, 2085 (2003).
[6] Y. Jong-ll, R. Klenz, and J. I. Kim, Appl. Spectrosc. **56**, 852 (2002).
[7] A. K. Knight, N. L. Scherbarth, D. A. Cremers, M. J. Ferris, Appl. Spectrosc. **54**, 331 (2000).
[8] S. K. Sharma, P. G. Luccy, M. Ghosh, H. W. Hubble, K. A. Horton, Spectrochim. Acta, Part A **59**, 2391 (2003).
[9] S. Kyuseok, L. Yong-lll, and J. Sneddon, Appl. Spectrosc. Rev. **32**, 183 (1997).
[10] E. Tognoni, V. Palleschi, M. Corsi, G. Cristoforetti, Spectrochim. Acta, Part B **57**, 1115 (2002).
[11] E. R. Runge, R. W. Minck, Spectrochim Acta Part B **20**, 733 (1964).
[12] D. A. Rusak, B. C. Castle, B. W. Smith, J. D. Winefordner, Trends Anal. Chem. **17**, 453 (1998).
[13] B. Nemet, L. Kozma, Spectrochim Acta Part B **50**, 1869 (1995).
[14] R. Jordan, D. Cole, J. G. Lunney, K. Mackay, D. Givord, Appl. Surf. Sci. **86**, 24 (1995).
[15] V. S. Burakove, A. F. Bokhonov, P. A. Naumenkov, M. I. Nedelko, N. V. Tarasenko, J. Appl. Spectrosc. **65**, 442 (1998).
[16] K. Song, H. Cha, J. Lee, I. Lee Yong, Microchem. **63**, 53 (1999).
[17] M. H. Hong, Y. F. Lu, S. K. Bong, Appl. Surf. Sci. **154**, 196 (2000).
[18] M. Kuzuya, H. Aranami, Spectrochim Acta Part B **55**, 1423 (2000).
[19] G. Abdellstif, H. Imam, Spectrochim Acta Part B **57**, 1155 (2002).

[20] M. A. Hafez, M. A. Khedr, F. F. Elasksher, Y. E. Gamal, Plasma Sources Sci. Technol. **12**, 5 (2002).
[21] Z. Chen, A. Bogaerts, J. Appl. Phys. **97**, 06305 (2005).
[22] Y. Li, C. Hu, H. Zhang, Z. Jiang, Z. Li, Appl. Opt. **48**, B105 (2008).
[23] J. A. Aguilera, C. Aragon, G. Cristoforetti, E. Tognoni, Spectrochim Acta Part B **64**, 689 (2009).
[24] X. Wang, S. Amoruso, J. Xia, J. Appl. Surf. Sci. **255**, 5211(2009).
[25] Y. Lee, S. P. Sawan, T. L. Thiem, Y. Teng, Snedden J. Appl. Spectrosc. **46**, 436 (1992).
[26] V. Kumar, R. K. Thareja, J. Appl. Phys. **67**, 3260 **(**1990**)**.
[27] E. G. Gamaly, A. V. Rode, B. Luther-Davies, J. Appl. Phys. **85**, 4213 (1999).
[28] A. Kramida, Yu. Ralchenko, Reader J., and NIST ASD Team (2018). NIST Atomic Spectra Database (ver. 5.5.6).
[29] M. Musadiq, N. Amin, Y. Jamil, M. Iqbal, M. A. Naeem, H. A. Shahzad, Inter. J. Eng. and Technol. **2**(1), 32 (2013).
[30] B. Rashid, S. Hafeez, N.M. Shaikh, M. Saleem, R. Ali, M. A. Baig, Int. J. Modern Phys. B **21**, 2697 (2007).
[31] M. Ying, Y. Xia, Y. Sun, M Zhao, Y. Ma, X. Liu, Y. Li, X. Hou, Laser Particle Beams **21**, 97 (2003).
[32] H. Lindner, K. H. Loper, D. W. Hahn, K. Niemax, Spectrochim Acta B **66**, 179 (2011).
[33] P. Stavropoulos, C. Palagas, G. N. Angelopoulos, D. N. Papamantellos, S. Couris, Spectrochim. Acta B **59**, 1885 (2004).
[34] H. R. Griem, Principles of Plasma Spectroscopy, Cambridge Uni. Press, Cambridge, 1997.
[35] Y. Lu, Z. Tao, M. Hong, J. Jpn. Appl. Phys. **38**, 2958 (1999).
[36] N. M. Shaikh, B. Rashid, S. Hafeez, Y. Jamil, M. A. Baig, J. Phys. D Appl. Phys. **39**, 1384 (2006).
[37] D. Gunther, S. E. Jackson, H. P. Longerich, Spectrochim Acta B **54**, 381 (1999).